CFD Modeling of Regular and Irregular Waves Generated by Flap Type Wave Maker

Ali Shehab[1,*], Ahmed M. R. El-Baz[2], Abdalla Mostafa Elmarhomy[1]

[1] Engineering Physics and Mathematics Dept., Faculty of Engineering, Ain Shams University in Egypt, Cairo 11517, Egypt
[2] Mechanical Engineering Dept., Faculty of Engineering, The British University in Egypt, Cairo, 11837, Egypt

ARTICLE INFO	ABSTRACT
	The improvement of wave generation in numerical tanks represents the key factor in ocean engineering development to save time and effort in research concerned with wave energy conversion. For this purpose, this paper introduces a numerical simulation method to generate both regular and irregular waves using Flap-Type wave maker. A 2D numerical wave tank model is constructed with a numerical beach technique, the independence of the numerical beach slope is tested to reduce the wave reflections. The different governing parameters of the Flap type wave maker were studied such as periodic time dependency and length of the flap stroke. The linear wave generated was validated against the wave maker theory WMT, the numerical results agreed with WMT. The Pierson-Moskowitz model is used to generate irregular waves with different frequencies and amplitudes. The numerical model succeeded to generate irregular waves which was validated against published experimental data and with Pierson-Moskowitz spectrum model using Fourier expansion theory in the frequency domain. Useful results are presented in this paper based on the numerical simulation to understand the characteristics of the waves. This paper produces a full guide to generate both regular and irregular waves numerically using ANSYS-CFX approach to solve the 2D Unsteady Reynolds Averaged Navier-Stokes Equation (URANS).

1. Introduction

The improvement of wave numerical simulation represents the key factor of the development and research of wave energy converters WECs. The increasing of renewable energy demand in the 20th century led to a revolution in the wave simulation specially in the last twenty years. The Numerical Wave Tank NWT is the general representation of the wave free surface motion and the hydrodynamic forces using numerical modelling. A good simulation of NWTs is very important for modelling of wave energy conversion devices which helps to improve efficiency and save cost and time instead of constructing expensive prototypes. Ocean engineering researchers in the recent

---

* Corresponding author.
E-mail address: alishehab2@eng.asu.edu.eg

decades made a great effort to develop the numerical tools required to optimize and refine the WECs designs [1].

The WECs simulations use the technique of Fluid Structure Interaction FSI coupled with the NWTs results to analyze the motion of the floating body. The partial differential equations governing the computational representation of NWTs I are the Reynolds Averaged Navier-Stokes Equation (RANS) which describe the transfer of mass and momentum. The governing differential equations of wave generation modelling usually solved based on three CFD techniques. ANSYS-fluent is used with a given code to generate the wave profile, AQWA is an easy way to generate a simple wave, ANSYS-CFX is the third way to produce NWT which helps to study a wide range of wave generation parameters [2].

The experimental work of wave generation started 60 years ago to improve the theoretical model of waves which is called the Boussinesq Equation BE. Researchers after that did a great effort to improve the design and construction of wave makers to increase the efficiency to generate regular and irregular waves experimentally. Eldrup and Andersen [3] presented a new model to generate regular and irregular waves. The second order wavemaker theory was modified for the purpose of reducing the spurious waves. The modified model gave an acceptable representation of the regular and irregular waves and the modified second-order wavemaker method is more relevant in irregular waves [3]. Khalilabadi and Bidokhti [4] construct a wave flume to produce both regular and irregular waves using flap-type wave maker, but only regular waves were presented. This wave maker is controlled by a computer, and a 1:4 sloped beach is used to absorb the wave reflections. The experimental results of wave height-to-stroke of the regular wave were compared with WMT by plotting the wave height to flap stroke ratio against the relative depth (kh), a good agreement was indicated [4]. Spinneken and Swan [5] developed a force-feedback control which concerns the wave generation using flap-type wave maker. The improved theory is limited only to generate regular waves [5]. Sénéchal and Dupuis [6] investigate the response of secondary waves in both breaking and nonbreaking conditions. The generated irregular wave is the sum of interacted pairs of waves. The elevation of each type of waves were presented against the time in both breaking and nonbreaking conditions [6]. Briggs *et al.,* [7] used a directional spectral wave generator to construct a 3D model study the diffraction of the wave against a breakwater. A multi-directional regular and irregular wave were simulated with different frequencies. 3D representation of the frequency spectrum was presented for irregular wave model [7]. Nwogu [8] derived a new form of BE which used to model the transformation of waves, the improved equations were solved using finite different method. This paper performed a numerical experiment of both regular and irregular waves to evaluate the ability of the improved form of BE in deep water and shallow water. This paper considers the JONSWAP spectrum to generate the sea state synthesized wave [8]. Ursell *et al.,* [9] construct an experimental wave tank to validate the WMT. The generated wave parameters in this paper were set based on LWT [9].

The previous CFD simulation work of wave generation used five different methods to generate NWT which are Relaxation zone, Static boundary, Dynamic boundary method, Mass source and Impulse source [1]. Most of the previous work in wave energy CFD modelling introduced the numerical techniques to study WECs. Less of these researches investigated the parameters affecting on the wave generation using CFD [19]. Finnegan and Goggins [10] used CFD to explore a numerical simulation of regular waves in both shallow and deep water. The numerical results were validated against both WMT and Linear wave theory LWT. The position of the flap-type hinge was raised to increase the restriction against the lower values of normalized wavenumber [10]. Lal and Elangovan [11] constructed a three-dimensional NWT using Ansys CFX viscous flow solver. The governing parameters affecting the behavior of flap-type wave maker were studied. Again, this paper

considered only the simulation of regular waves with varies wavelength and amplitude. The numerical results were validated against WMT and gave a good agreement [11]. The improvement of the theoretical techniques in wave simulation has been performed in most previous research. Ning and Teng [12] developed a fully nonlinear irregular NWT. The numerical method used an integral equation form to solve the Laplace equation in each time step. This method is applicable in simulating both regular and irregular waves. The results were validated with the theoretical values [12].

The present paper focuses on the regular and irregular wave simulations in a wide range of water depth and wave amplitude. The WMT of regular waves in the previous work were found not applicable in deep water regions at which the normalized wavenumber kh is less than 3.14 based on LWT when the flap-type wavemaker is hinged at the seabed [13]. A good simulation of the sea surface wave is made by adding a lot of regular waves, this is called random linear wave theory [14]. The numerical simulation of irregular waves using CFD is a new approach in this paper using flap-type wave maker. There are two different schemes of irregular wave spectrum, Jonswap and Pierson-Moskowitz spectrum models. In the present investigation, the results are compared with both models.

2. Methodology and Problem Setup

The main purpose of this paper is to conduct a numerical simulation of the different types of waves using CFD. Most of the previous work in this field presented brief studies to simulate the linear waves. This paper improves the previous methods in linear wave simulation and present a numerical method to simulate the irregular waves using ANSYS-CFX (release 14.5) approach [2].

The motion of the Flapper is directly affecting the wavelength of the generated waves. In the present work, the dependence of the numerical wave height and wavelength on the flap stroke length is studied. A sum of regular plane waves with different frequencies and amplitudes based on Pierson-Moskowitz spectrum model was used to generate the irregular wave equation. The frequency domain of the generated wave was validated with Pierson-Moskowitz spectrum model.

The CFD model used in the present work is shown in Figure 1. A 2-dimensional multi-phase model is constructing using ANSYS modeler with three different regions as shown. Phase one, in the upper region, is air with a density is specified to be 1.185 kg/m³ at 25° temperature. The second phase in the lower region is water with a density is specified to be 997 kg/m³ at 25° temperature. The two phases are coupled using volume fraction coupling technique at the free surface of the sea [2].
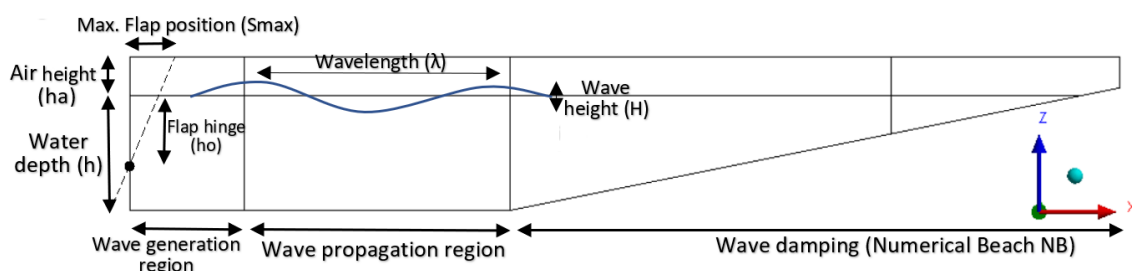
Fig. 1. Numerical wave tank model

The model is divided into three different regions. First one is the wave generation region, in which the wave is generated using Flap-type wave maker applied at the left side of this region. The length of the wave generation region is recommended to be equal to the water depth as a minimum value to give a smooth dynamic mesh in this area. The second region is the wave propagation region in which the wave considered to be steady. Most of the previous researches in WECs recommended to

place the device within this stage [15]. At the end of the wave propagation region, a numerical beach NB is placed to absorb the wave at the end of the model and reduce the wave reflections. The numerical wave tank was constructed using a proper dimension based on the linear wave theory LWT. The air hight (ha) inside the wave tank is set to be 1/3 of the water depth (h) as a minimum value according to WMT [10].

2.1 Mathematical Model

The free surface flow of water is an unsteady incompressible flow. The governing equations needed to be solved is continuity equation for the velocity problem (1) and (2) and momentum equation for the pressure problem (3) and (4).

Continuity equation

$$\nabla.(\vec{v}) = 0 \tag{1}$$

$$\vec{v} = u\hat{i} + w\,\hat{k} \tag{2}$$

where $\vec{v}$ represents the velocity vector. u and w are the components of velocity in x and z directions respectively, ρ is the fluid density, and t is time. [16]

Momentum equation

$$\rho\left(\frac{\partial u}{\partial t} + u\frac{\partial u}{\partial x} + w\frac{\partial u}{\partial z}\right) \\ = -\frac{\partial P}{\partial x} + 2\mu\frac{\partial^2 u}{\partial x^2} + \frac{\partial}{\partial z}\left(\mu\left(\frac{\partial u}{\partial z} + \frac{\partial w}{\partial x}\right)\right) + F_i \tag{3}$$

$$\rho\left(\frac{\partial w}{\partial t} + u\frac{\partial w}{\partial x} + w\frac{\partial w}{\partial z}\right) \\ = -\frac{\partial P}{\partial z} + 2\mu\frac{\partial^2 w}{\partial z^2} + \frac{\partial}{\partial x}\left(\mu\left(\frac{\partial u}{\partial z} + \frac{\partial w}{\partial x}\right)\right) \\ + F_k - \rho g \tag{4}$$

where x and z are the horizontal and vertical positions of the point of interest with respect to the origin which placed on the sea water level SWL at the inlet side "Flapper", u and w are the horizontal and vertical components of the velocity along x and z axes respectively, F_i and F_k are the horizontal and vertical forces on the fluid directed along the x and z axes respectively, P is the pressure of the fluid, the term ρg represents the gravitational force of the fluid element, μ is the viscosity [16].

The previous two general equations continuity and momentum are to be solved using Finite Volume Method FVM by ANSYS CFX software [2]. FVM have generally been applied to research on complex fluid flow due to the development of computers, since it can give a clear vision into the physics of the flow. The key step of FVM is the integration of the governing equations over a control volume, yields the discretized equation. The first step that should precede discretization is to divide the computational domain into discrete control volumes.

Another governing equation added to the model for the solution of the volume fraction VF of the fluids in order to determine the vertical position of the free surface at any time (5) to (7). This method is called "volume of fluid method VOF" derived by Liang *et al.,* [17].

$$\frac{\partial(q_a)}{\partial t} + u\frac{\partial(q_a)}{\partial x} + w\frac{\partial(q_a)}{\partial z} = 0 \tag{5}$$

$$\frac{\partial(q_w)}{\partial t} + u\frac{\partial(q_w)}{\partial x} + w\frac{\partial(q_w)}{\partial z} = 0 \tag{6}$$

$$q_a + q_w = 1 \tag{7}$$

where q_a and q_w are the volume fraction of the two phases used in the model air and water respectively. The position of the free surface in z direction is determined by integrating the volume fraction with respect to dz, this technique gives the minimum value of q_a- q_w [20].

2.2 Boundary Conditions

Boundary conditions used in this study on the two phases air and water are

(i)   The inlet is set to be Flapper with variable x position depends on the z-displacement and time according the equation

$$X = S_{max} * \frac{Z + h_o}{h_a + h_o} \tag{8}$$

where X is the horizontal position of the points of the flapper at any vertical position Z, h_o is the depth of the flap hinge from SWL as shown in Figure 1, h_a is the air Hight, S_{max} is the flap position at the top surface of the model which is subjected to a single sin wave as a function of time to produce a regular wave for the free surface define as followed

$$S_{max} = A_f \sin(\omega t) \tag{9}$$

where A_f is the maximum flap amplitude at the top of the model, ω is the angular velocity of the flapper based on the desired wave which defined by Eq. (10) [13]:

$$\omega^2 = gk \tanh(kh) \tag{10}$$

where the term (kh) is called the normalized water depth, h is the water depth, k is the wave number defined by Eq. (11)

$$k = 2\pi/\lambda \tag{11}$$

where λ is the wavelength of the desired wave, the efficiency of the flapper to generate the desired wave is characterized by the Eq. (12) according to WMT [13]

$$\frac{H}{S_o} = 4\left(\frac{\sinh kh}{kh}\right)\frac{kh \sinh kh - \cosh kh + 1}{\sinh 2kh + 2kh} \tag{12}$$

where H is the wave Height, so is the total flap stroke at the SWL (Z=0) as define in Eq. (13), the (H/S_o) term in Eq. (12) is called height-to-stroke ratio which could be simplified in case of shallow water, to Eq. (14) [13]

$$S_o = 2 * A_f * \frac{h_o}{h_a + h_o}$$

(13)

$$\frac{H}{S_o} = \frac{kh}{2}$$

(14)

(ii)   The outlet is set to be opening with a static pressure.

(iii)   The upper side is divided into two regions, first one nearest the flapper is an opening specified with a dynamic mesh, second region is an opening with 0 static pressure.

(iv)   The seabed is divided into two regions, first one nearest the flapper is a wall with no slip condition specified with a dynamic mesh, second region is a wall with no slip condition.

2.3 Grid Generation

The model is discretized into finite elements using ANSYS design modeler. The elements are in structured rectangular shapes as shown in Figure 2. Some triangular elements appear at the end of the model in order to cover all area enclosed by the numerical beach with acceptable skewness. The elements are refined near the free surface in order to capture the small movements of the fluid. The longitudinal axis at the free surface is divided onto elements with varies size to check independency.
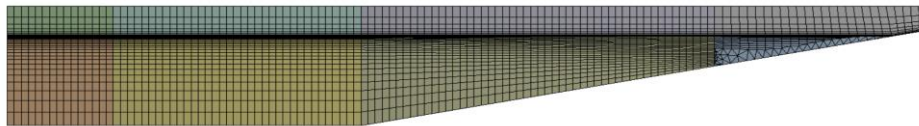
Fig. 2. Two-dimensional mesh of the model

2.4 Grid Independence Test

Ten cases are generated with different mesh parameters to check the independence of mesh with a proper NB slope, the wave elevation in z direction is plotted against time for this purpose, Figure 3. The periodic time used in this test is 1.38 sec, from Eq. (10), at water depth 1.5m and wavelength 3m. Figure 4 shows the change of wave Height H against the grid growth. The acceptable number of elements selected to be 4000 with minimum cell size 0.1m at the free surface, the change of wave height doesn't exceed 0.9% of that at 6000 elements.
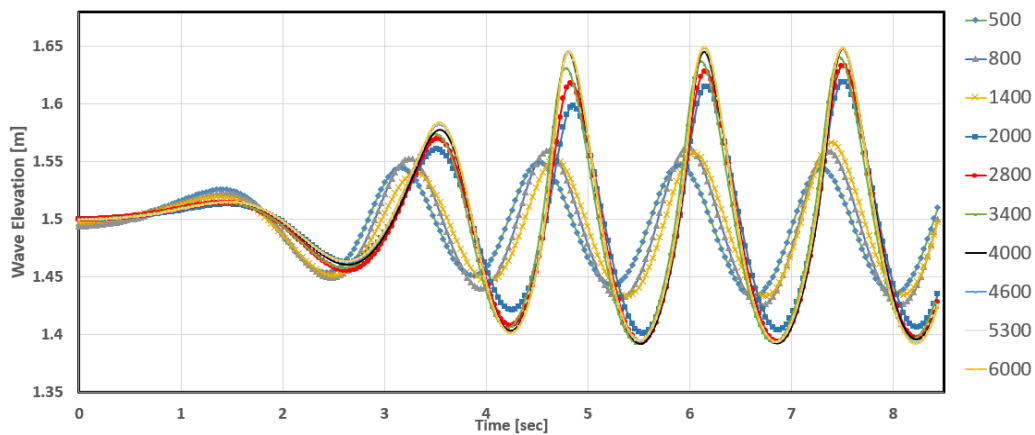
Fig. 3. Grid independency test (wave elevation)
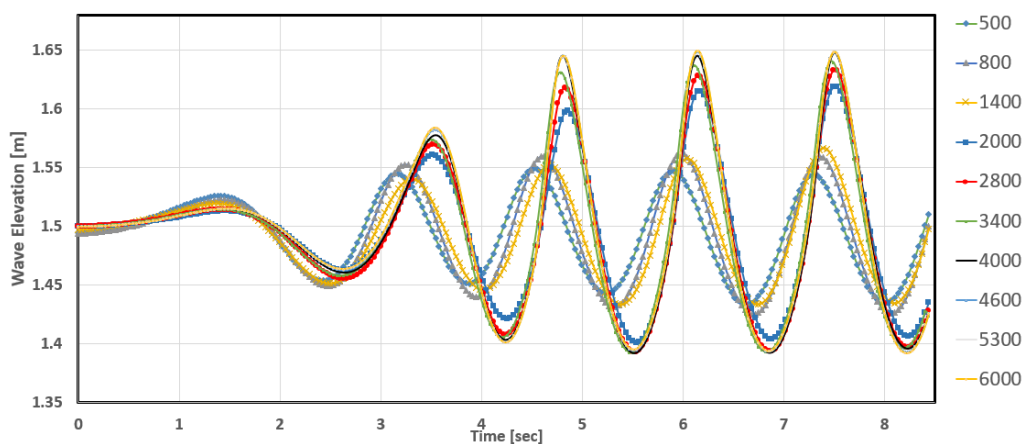
Fig. 4. Grid independency test (wave amplitude)

2.5 Domain Test

To study the effect of the model domain on the generation and stability of the wave, five different models are generated with laminar flow and the transient first order scheme is selected to solve the differential equations. All cases have the same numerical beach slope, only the distance from the flapper to the start of NB is changed from 2h to 6h, h is the water depth set to 1.5m in this test. Figure 5 shows the change of wave elevation against time in each case. The results are stable at the different positions of NB with inconsiderable deviation, 3h and 4h have the same error 0.8% with respect to 6h as shown in Figure 6, the domain 3h is selected to save time of calculation.
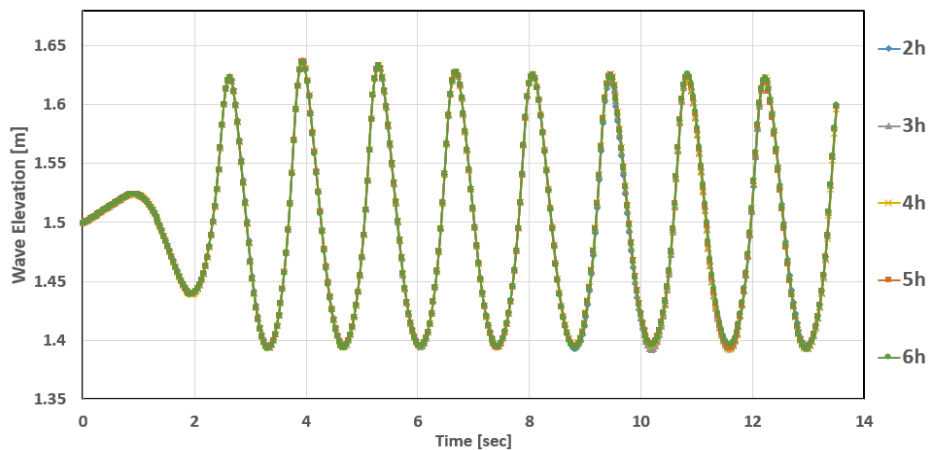
Fig. 5. Wave elevation at a distance 2h from the flapper (Domain Test)
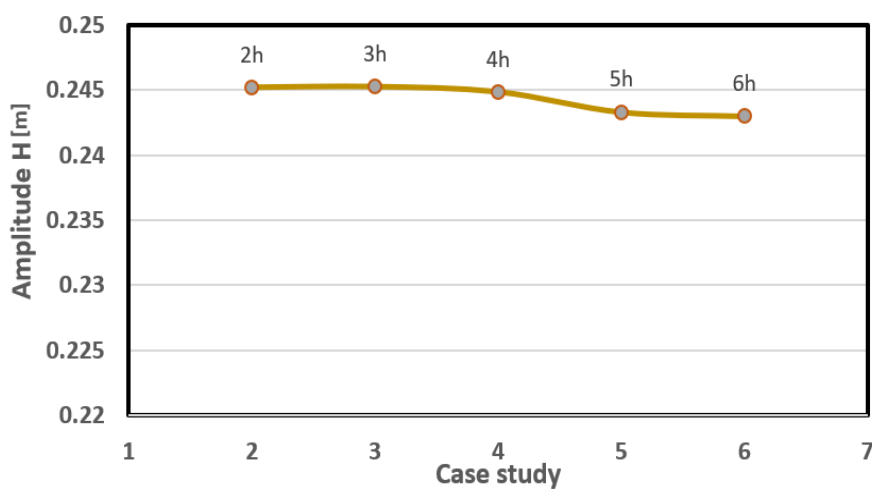
Fig. 6. Wave amplitude at a distance 2h from the flapper (Domain Test)

2.6 Time Step Size Test

Selecting of the time step size of calculations effects on the response of flapper motion and generated wave. Figure 7 shows the change in wave amplitude against the time step size ratio, equal to the periodic time divided by the time step size, at two different periodic time 1.38 sec and 2 sec. at same water depth h=1.5m. the wave amplitude shown in Figure 7 is calculated from a distance 3h from the flapper. It is shown that T/60 and T/70 for time step size gives an acceptable result with a deviation about 1.5% and 0.8% respectively. This agrees closely to William Finnegan and Goggins [10] which recommended to divide the periodic time to 50 divisions T/50. Ning and Teng [12] recommended to use T/40 for time step size, this ratio gives an error 6% in both periodic times shown in Figure 7. This study recommended to divide the periodic time into 60 divisions instead of (T/50) which could be used with error 3%.
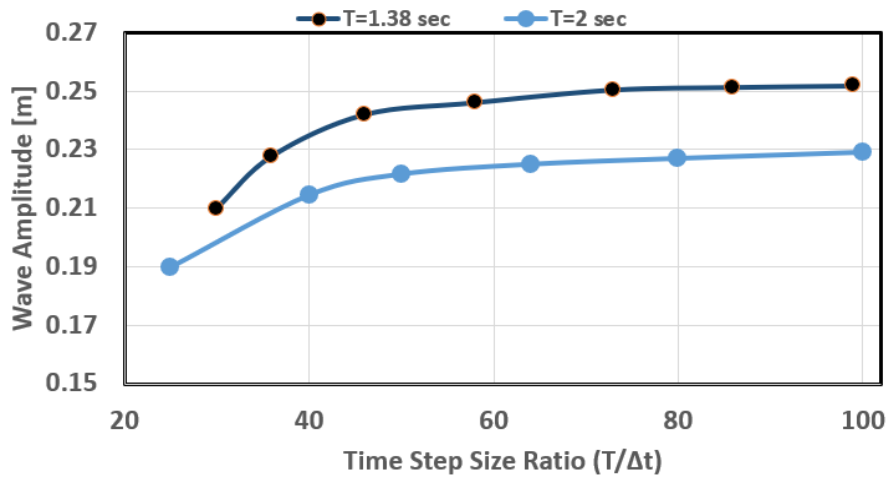
Fig. 7. Time step size dependency at same water depth

2.7 Numerical Beach Slope Test

A lot of researches made a great effort in order to reduce the wave reflections from the model outlet. Liang *et al.,* [17] added a source term in the momentum equation which contributed to reduce reflection of the generated wave. In this study, NB with a specific slope is constructed at the end of the model to dissipate the generated wave and reduce reflections. Seven cases were investigated for this test, first one the domain has no NB. Other cases, the slope of NB varies from 1:1 to 1:6 with same water depth h=1.5m, total domain of the model is set to be 9h. the generated wave has a periodic time 1.38 sec and wavelength 3m. the model is considered to be deep water due to the normalized water depth kh = 3.14 based on LWT which is valid for kh ≥ 3.13 [13]. The stroke length of the flapper at the SWL is 0.45m in this test. Figure 8 shows the comparison of wave elevation against time at a distance h from the end of the model for all seven cases. It is shown that the increasing of NB slope tends to a slight reduction in wave displacement near the beach.
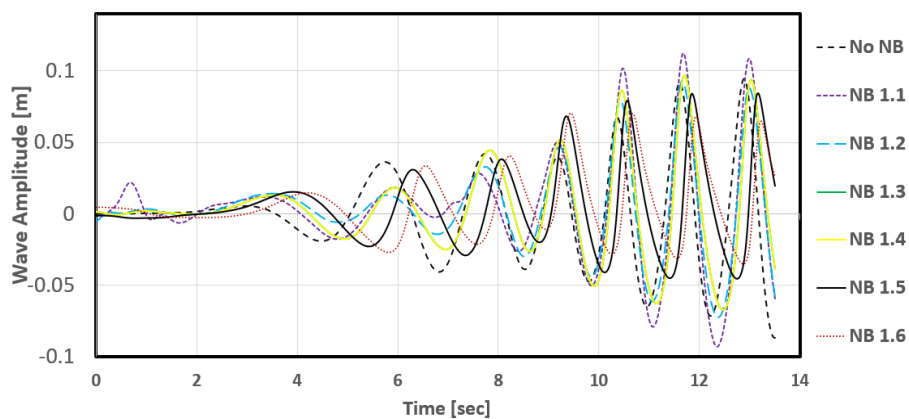
Fig. 8. Wave amplitude at distance h from the outlet at different NB slopes

Wave amplitude in each case is shown in Figure 9, slope 1:5 and 1:6 of NB shows a better reduction in wave amplitude at h distance from the end of the model which tends to reduce wave reflections. Figure 10 shows the free surface profile along the longitudinal axis of the model to detect the effect of using NB technique. Some oscillations are appeared at the end of the model, the ability of using NB technique is shown in Figure 11 which shows the damping coefficient of the generated wave in each slope of NB. The damping coefficient is defined by [18]:

$$A = A_p e^{-C_d X} \sin(\omega t + \lambda X)$$

(15)

where A_p is the peak amplitude of the wave could be shown in Figure 10, A is the wave amplitude at any time t and position X, C_d is the damping coefficient of the generated wave. From this study, 1:5 numerical beach slope is selected.
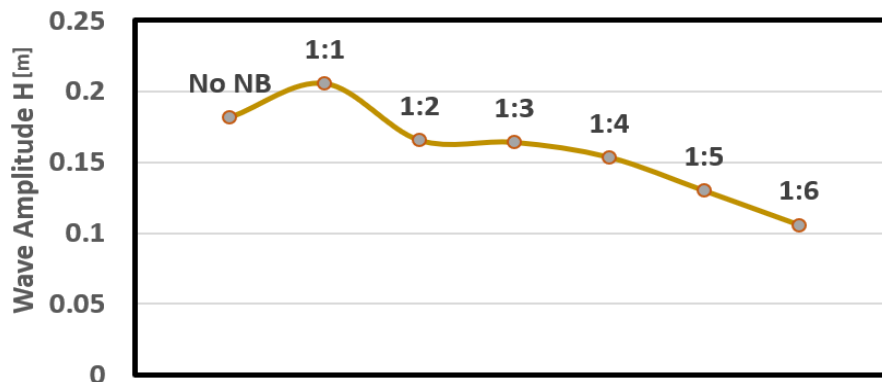
Fig. 9. NB slope independent test at a distance h from the outlet
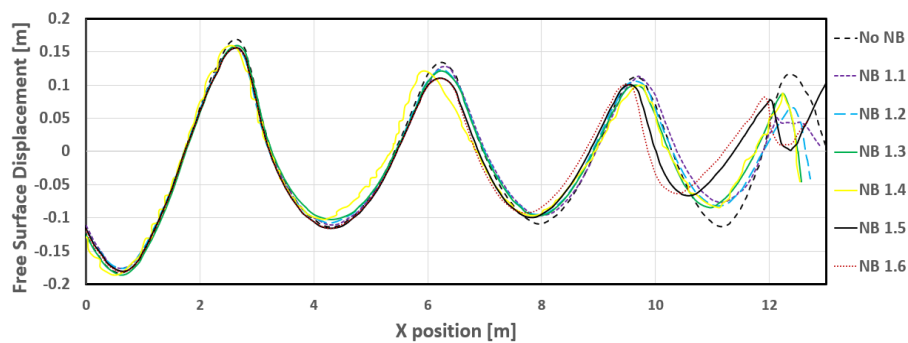
Fig. 10. Free surface displacement along the x direction after 10 cycles
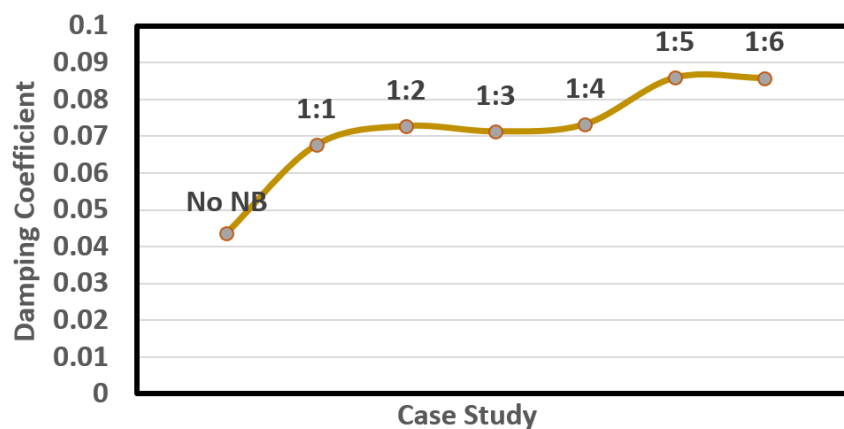
Fig. 11. Wave damping coefficient due to using Numerical Beach

2.8 Stability of the Generated Wave

The generated wave takes required a period to be stable as the theoretical wave profile. Three different waves were generated for this purpose as shown in Figure 12. Each wave profile was presented against the number of cycles within the first 10 cycles, Figure 12 shows that each wave

required 4 cycles to be stable. This result will be used later in irregular wave simulation to spot the real action of sea wave spectrum [21].
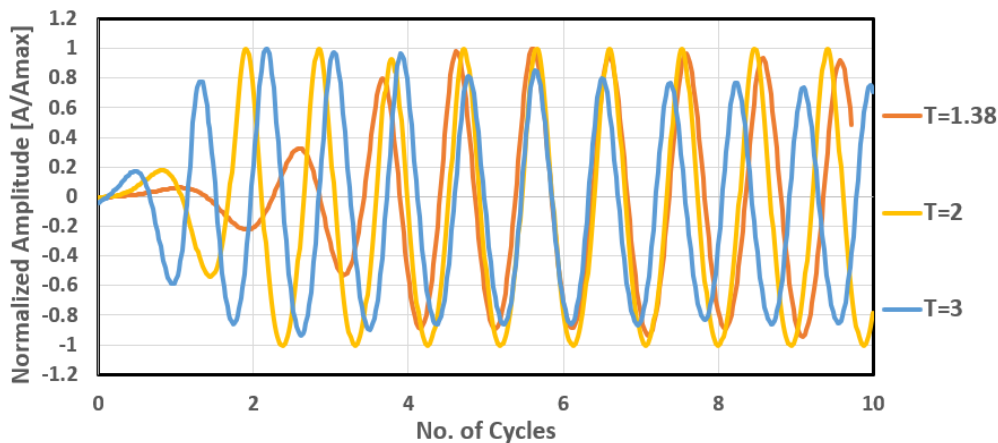
Fig. 12. Wave stability against the number of cycles at three different periodic time

2.8 Validation of the Numerical Results

The numerical results are validated against WMT at different solution methods of the differential equations. All the previous recommendations were taken in consideration in the final validation. 1st order and 2nd order of the transient schemes for both continuity and momentum equations were validated against Wave Maker Theory WMT, Figure 13, at periodic time 1.38 sec. The 2nd order model is shown to be more closely to the standard WMT after 4 cycles. From the presented study, this paper introduces a simple method to simulate the regular waves and recommended the general parameters for this approach. The proper geometry of the model and wave parameters selected in this paper gave an agreement against the wave theories. The study of the regular wave characteristics and the performance of the numerical model is presented in the next sections.
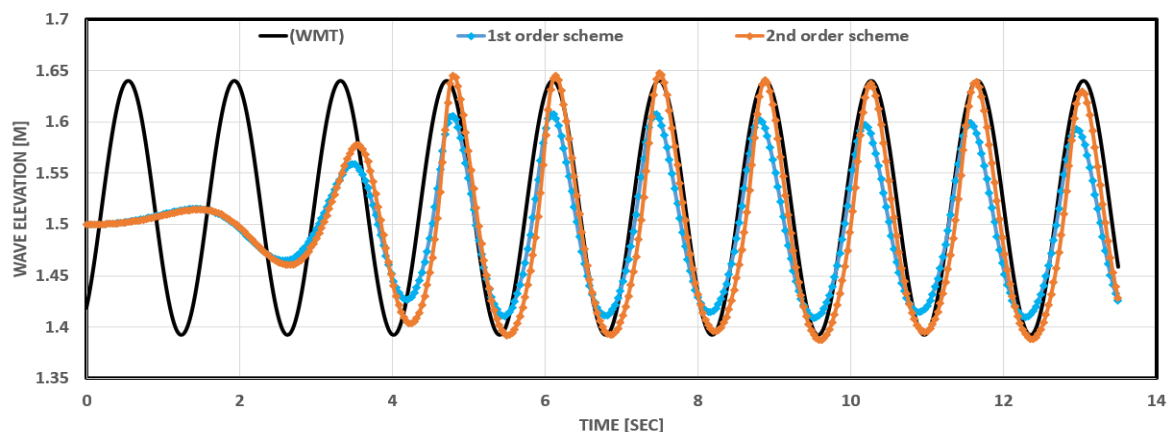
Fig. 13. Validation of the numerical results against WMT

3. Results and Discussion

The relation between the normalized Flap stroke and the generated wavelength is an effective parameter that affects the extent of convergence with the real sea wave. This study helps to increase the efficiency of the numerical wave tank by selecting the proper Flap stroke length. This is an

important note, which determine the value of So at different wavelength and periodic time T. The wave will be more stable and tends to be symmetric about WSL. Two different studies were generated with different periodic time, first study with 1.388 sec at Deep water case which the value kh is 3.14 and the Flap is hinged at the seabed. Figure 14 shows the change of height-to-stroke ratio against the normalized wavelength at water depth 1.5m and wavelength 3m. It is clear to say that at deep water case the best value of Flap stroke length is 1/25 of the wavelength which give a minimum deviation from WMT. The second study is set with 2 sec periodic time at Shallow water case which the value kh is 1.26 and the Flap is hinged at the seabed, the water depth is 1.2m and the wavelength is 6m to achieve the case of Shallow water. Figure 15 shows that the wave is more stable at law values of S in case of shallow water when the value of the stroke length So is 1/20 of the wavelength. The variation of the amplitude is decreased. Moreover, the value of H/S is closer to WMT.
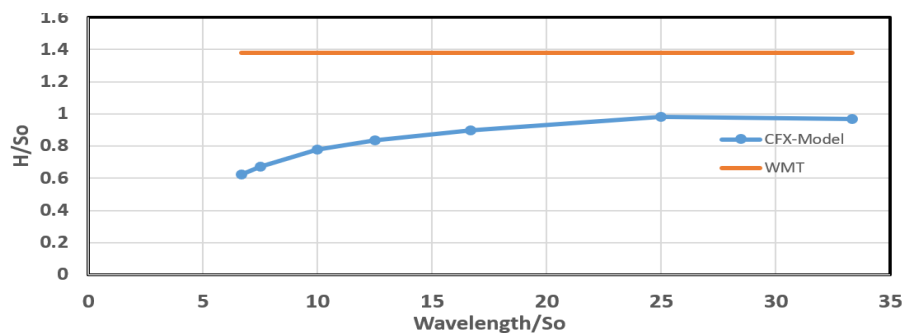
Fig. 14. Flap Stroke dependence in case of Deep water at kh=3.14
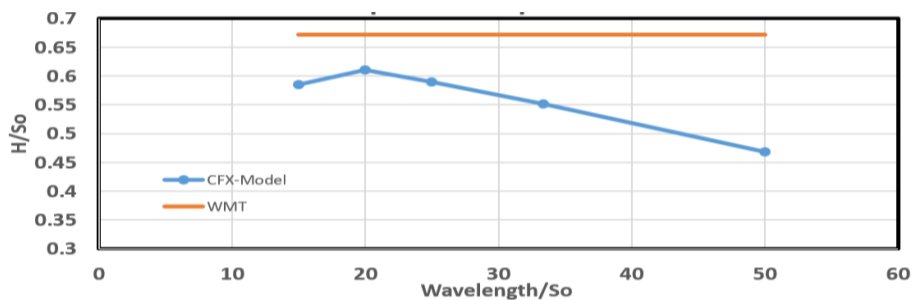
Fig. 15. Flap Stroke dependence in case of Shallow water at kh=1.26

The efficiency of the numerical wave tank is tested by comparing the CFD results against WMT and the previous work done by Finnegan and Goggins [10]. Figure 16 shows the relation between the height-to-stroke ratio H/S and the relative depth kh, the Flap in this study is hinged at the seabed. The numerical model succeeds to predict the desired wave parameters in case of Shallow water at which the relative depth kh is less than 3.13 according to LWT. In case of Deep water, the CFD results doesn't satisfy the WMT. This issue could be eliminated by changing the position of the flap hinge instead of the seabed position [20].
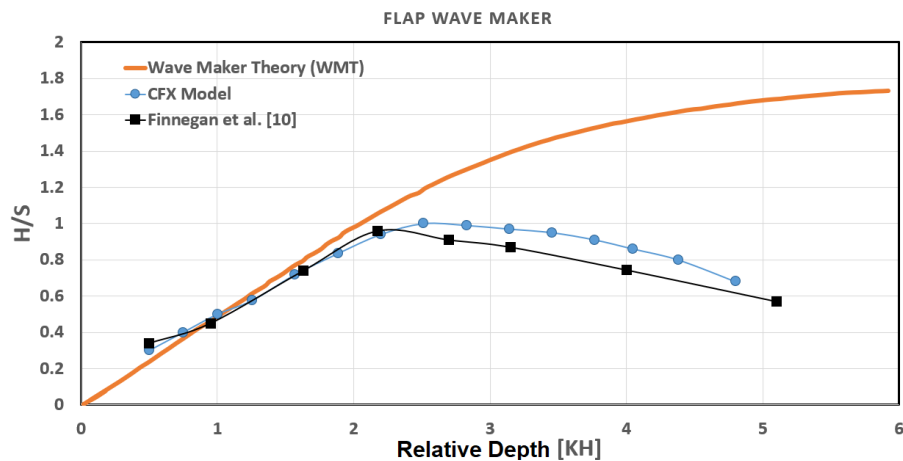
Fig. 16. Validation of CFD results against WMT and previous work

3.1 Irregular Wave Simulation

The numerical simulation of the irregular waves was a great challenge for researchers in the field of wave energy. This paper introduces a numerical method to simulate the irregular wave using Flap-type wave maker in CFX. The wave spectrum model developed by Pierson-Moskowitz was used in this study to validate the numerical results. Pierson-Moskowitz model define the spectral density of the wave by

$$S(f) = Ae^{-B/f^4} / f^5 \tag{16}$$

where f is the wave frequency, A and B are constants related to the wind speed above the sea water level, and to the main sea state parameters which defined by:

$$A = \frac{5}{16} Hm0^2 f_p^4$$
$$B = 5f_p^4 / 4 \tag{17}$$

where Hm0 is the significant wave height and f_p is the peak frequency at which the maximum wave amplitude exists. In this study, the peak frequency is set to be 0.72 Hz and the significant wave height 0.5m. The methodology followed in this paper to generate the irregular wave is to use the Pierson-Moskowitz model for producing a series of regular sine waves with different frequencies and amplitudes on the form

$$H = \sum_{i=0}^{20} a_i \sin(\omega_i t + \varphi_i) \tag{18}$$

where ω is the angular velocity which is equal to $2\pi f$, and φ_i is the phase shift angle which set to be 0 in this model. the selected amplitudes and frequencies were converted to its corresponding values to be applied on the Flap stroke variation by the recommended ratios shown in regular wave model in this paper. The total time is set to be 30 sec. with time step size of 0.02 sec which is recommended before in regular wave simulation. The generated wave elevation is presented against time at 3d away from the Flap, Figure 17.
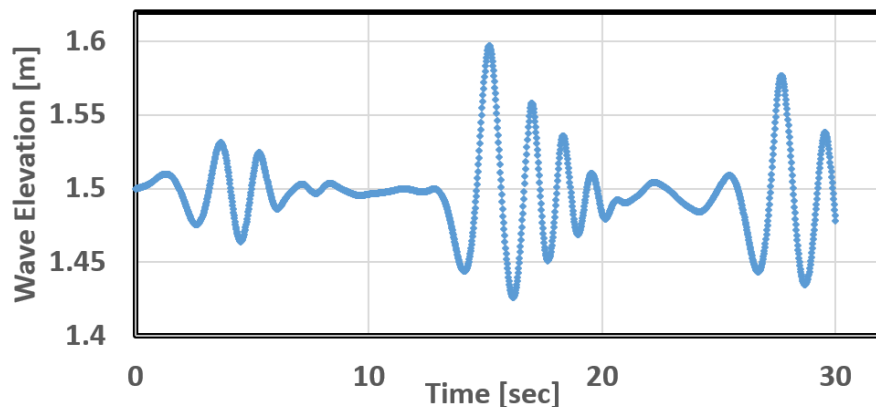
Fig. 17. Time domain of the generated irregular wave (Pierson-Moskowitz)

3.2 Validation of the Numerical Results

The irregular wave generated in this paper is validated against the Pierson-Moskowitz model in the dimensionless frequency domain to check the ability of the CFD model to predict the real sea wave spectrum. The Cartesian data shown in Figure 17 is converted into the frequency domain using Fast Fourier Transform after eliminating the first 4 cycles of the wave to ensure the stability of the generated wave. Figure 18 shows the dimensionless frequency domain of the CFX model comparing with the irregular wave spectrum by Pierson-Moskowitz. The numerical CFD model succeeds to generate an irregular wave which is validated against Pierson-Moskowitz spectrum model using Fourier expansion theory in the frequency domain, Figure 18.
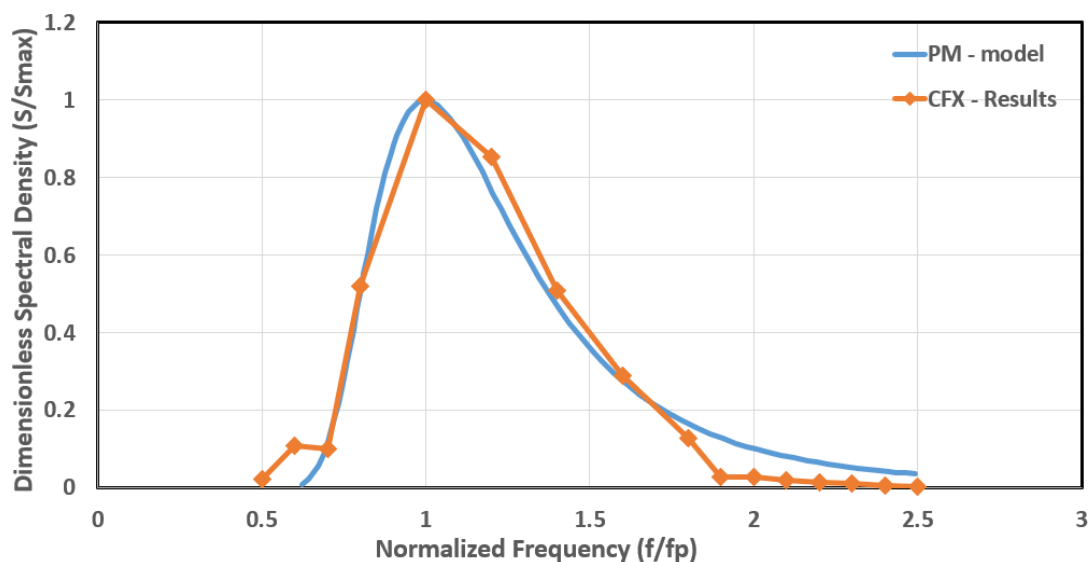
Fig. 18. The frequency domain of the irregular wave (Pierson-Moskowitz)

Another irregular wave model was used in this study to validate the numerical results called JONSWAP spectral model. JONSWAP model defines the spectral density of the wave by Eq. (19) which is thus spectral density of Pierson-Moskowitz model multiplied by additional term called "Peak enhancement factor"

$$S(f) = S_{PM}(f)\gamma^{\exp\left(-(f-f_p)^2/(2\sigma^2 f_p^2)\right)}$$

(19)

The same procedure was followed to generate an irregular wave using JONSWAP model. The time domain of the wave is presented in Figure 19 with total time 30 sec and the water depth is 1.5m. The numerical results are validated against the theoretical model of JONSWAP and also compared with the experimental data published by Nwogu [8] with water depth 0.2m, Hm0 is 0.09m, peak frequency of 0.67 Hz, and γ is 3. Figure 20 shows the dimensionless frequency domain of the generating irregular wave. The numerical results show a wave spectrum which is close to the mathematical model.
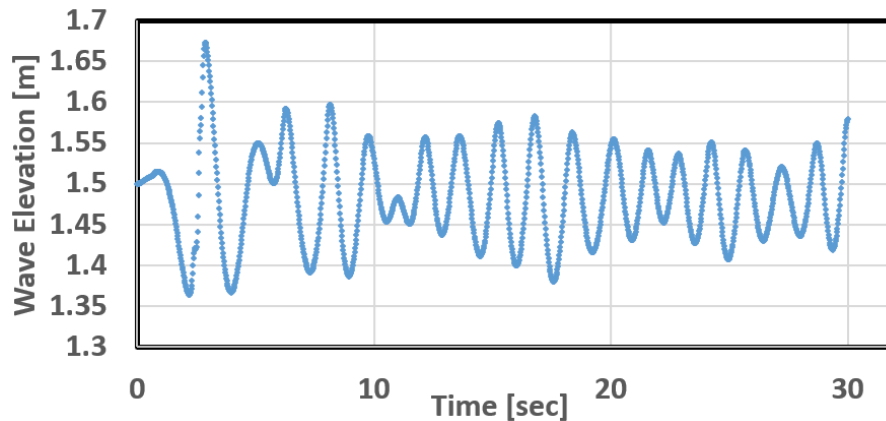
Fig. 19. Time domain of the generated irregular wave (JONSWAP)
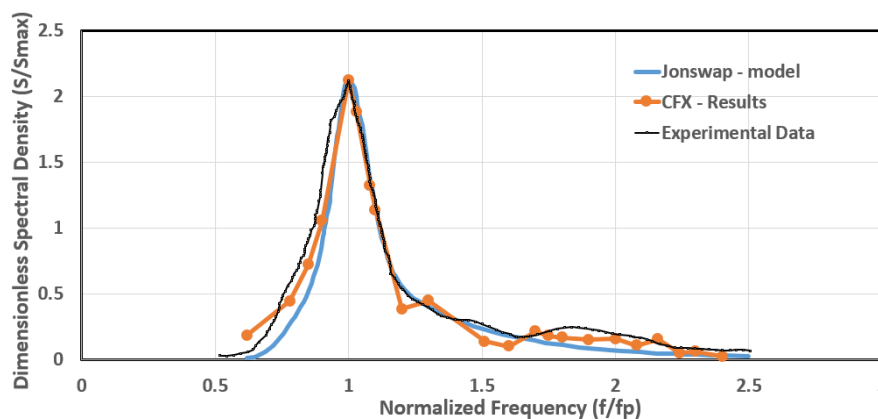
Fig. 20. The frequency domain of the irregular wave (JONSWAP). Experiments are in reference [8]

4. Conclusion

Two different models were generated using ANSYS-CFX to simulate both regular and irregular waves. A Flap-type wave maker was used for this purpose. This paper introduces some recommendations to select the different parameters affecting on the efficiency of Flap-type wave maker. The ratio of the maximum stroke length of the Flap and the desired wavelength is recommended to be 1/25 in case of Deep-water regular wave model, this value is 1/20 in case of Shallow-water regular wave. The time step size is recommended to be at least 1/70 of the periodic time. The numerical beach slope was tested in this paper and recommended to be at least 1:5 which shows a better damping of the wave close to the beach. The generating regular wave stability was investigated, and the numerical results show that the wave needs a complete four cycles to be a stable. The linear wave generated was validated against the wave maker theory WMT, the numerical results agreed with WMT.

The numerical irregular wave is generated in this paper using a mathematical approach based on two different wave spectrum models, first is Pierson-Moskowitz model and second is JONSWAP model. The numerical results of the generated irregular wave were validated with a published experimental data with the same conditions. The method showed successful wave generation for both regular and irregular waves.

References

[1] Windt, Christian, Josh Davidson, and John V. Ringwood. "High-fidelity numerical modelling of ocean wave energy systems: A review of computational fluid dynamics-based numerical wave tanks." *Renewable and Sustainable Energy Reviews* 93 (2018): 610-630. https://doi.org/10.1016/j.rser.2018.05.020

[2] ANSYS. *ANSYS-CFX, Release 14.5*. ANSYS Inc., 2012.

[3] Eldrup, Mads Røge, and Thomas Lykke Andersen. "Applicability of nonlinear wavemaker theory." *Journal of Marine Science and Engineering* 7, no. 1 (2019): 14. https://doi.org/10.3390/jmse7010014

[4] Khalilabadi, M. R., and A. A. Bidokhti. "Design and Construction of an Optimum Wave Flume." *Journal of Applied Fluid Mechanics* 5, no. 3 (2012): 99-103.

[5] Spinneken, Johannes, and Chris Swan. "Second-order wave maker theory using force-feedback control. Part II: An experimental verification of regular wave generation." *Ocean Engineering* 36, no. 8 (2009): 549-555. https://doi.org/10.1016/j.oceaneng.2009.01.007

[6] Sénéchal, N., P. Bonneton, and H. Dupuis. "Field experiment on secondary wave generation on a barred beach and the consequent evolution of energy dissipation on the beach face." *Coastal Engineering* 46, no. 3 (2002): 233-247. https://doi.org/10.1016/S0378-3839(02)00095-9

[7] Briggs, Michael J., Edward F. Thompson, and Charles L. Vincent. "Wave diffraction around breakwater." *Journal of Waterway, Port, Coastal, and Ocean Engineering* 121, no. 1 (1995): 23-35. https://doi.org/10.1061/(ASCE)0733-950X(1995)121:1(23)

[8] Nwogu, Okey. "Alternative form of Boussinesq equations for nearshore wave propagation." *Journal of Waterway, Port, Coastal, and Ocean Engineering* 119, no. 6 (1993): 618-638. https://doi.org/10.1061/(ASCE)0733-950X(1993)119:6(618)

[9] Ursell, Fritz, Robert George Dean, and Y. S. Yu. "Forced small-amplitude water waves: a comparison of theory and experiment." *Journal of Fluid Mechanics* 7, no. 1 (1960): 33-52. https://doi.org/10.1017/S0022112060000037

[10] Finnegan, William, and Jamie Goggins. "Numerical simulation of linear water waves and wave-structure interaction." *Ocean Engineering* 43 (2012): 23-31. https://doi.org/10.1016/j.oceaneng.2012.01.002

[11] Lal, Anant, and Muniyandy Elangovan. "CFD simulation and validation of flap type wave-maker." *World Academy of Science, Engineering and Technology* 46, no. 1 (2008): 76-82.

[12] Ning, D. Z., and Bin Teng. "Numerical simulation of fully nonlinear irregular wave tank in three dimension." *International Journal for Numerical Methods in Fluids* 53, no. 12 (2007): 1847-1862. https://doi.org/10.1002/fld.1385

[13] Dean, Robert G., and Robert A. Dalrymple. *Water wave mechanics for engineers and scientists*. Vol. 2. World Scientific Publishing Company, 1991. https://doi.org/10.1142/1232

[14] Krogstad, Harald E., and Øivind A. Arntsen. "LINEAR WAVE THEORY PART A, Regular waves." *Lecture notes, Norwegian University of Science and Technology*, Trondheim, Norway (2000).

[15] Büchner, Anna, Thomas Knapp, Martin Bednarz, Philipp Sinn, and Arndt Hildebrandt. "Loads and Dynamic Response of a Floating Wave Energy Converter due to Regular Waves from CFD Simulations." In *International Conference on Offshore Mechanics and Arctic Engineering*, vol. 49934, p. V002T08A060. American Society of Mechanical Engineers, 2016. https://doi.org/10.1115/OMAE2016-54784

[16] Versteeg, Henk Kaarle, and Weeratunge Malalasekera. *An introduction to computational fluid dynamics: the finite volume method*. Pearson education, 1995.

[17] Liang, Xiu-feng, Jian-min Yang, Jun Li, Long-fei Xiao, and Xin Li. "Numerical simulation of irregular wave-simulating irregular wave train." *Journal of Hydrodynamics* 22, no. 4 (2010): 537-545. https://doi.org/10.1016/S1001-6058(09)60086-X

[18] Pata, Vittorino, and Marco Squassina. "On the strongly damped wave equation." *Communications in Mathematical Physics* 253, no. 3 (2005): 511-533. https://doi.org/10.1007/s00220-004-1233-1

[19] Ramli, Nurul Azihan, Azlin Mohd Azmi, Ahmad Hussein Abdul Hamid, Zainal Abidin Kamarul Baharin, and Tongming Zhou. "Effect of Cylinder Gap Ratio on The Wake of a Circular Cylinder Enclosed by Various Perforated Shrouds." *CFD Letters* 13, no. 4 (2021): 51-68. https://doi.org/10.37934/cfdl.13.4.5168

[20] Gupta, Ankit Kumar, Bhupendra Gupta, Jyoti Bhalavi, Prashant Baredar, Hemant Parmar, and Ramalingam Senthil. "CFD study on heat transfer and pressure drop of nanofluids (SiO_2/H_2O, Al_2O_3/H_2O, $CNTs/H_2O$) in a concentric tube heat exchanger." *International Journal of Ambient Energy* (2021): 1-16. https://doi.org/10.1080/01430750.2021.1913222

[21] Salleh, Nursyaira Mohd, Mohamad Shukri Zakaria, Mohd Juzaila Abd Latif, and Adi Azriff Basri. "A Computational Study of a Passive Flow Device in a Mechanical Heart Valve for the Anatomic Aorta and the Axisymmetric Aorta." *CFD Letters* 13, no. 4 (2021): 69-79. https://doi.org/10.37934/cfdl.13.4.6979